EPJ Web of Conferences **140**, 14001 (2017) DOI: 10.1051/epjconf/201714014001
Powders & Grains 2017

Enhancement of CO_2 capture in limestone and dolomite granular beds by high intensity sound waves

Jose Manuel Valverde[1,⋆], *Jose Manuel* Perez-Ebri[1], and *Miguel Angel* Sanchez-Quintanilla[1]

[1] *Faculty of Physics*
University of Seville
Ada. Reina Mercedes s/n 41012 Seville, Spain

Abstract. The calcium looping (CaL) process, based on the calcination/carbonation of $CaCO_3$ at high temperatures, has emerged in the last years as a potentially low cost technology for CO_2 capture. In this work, we show that the application of high intensity sound waves to granular beds of limestone and dolomite in a CaL reactor enhances significantly their multicycle CO_2 capture capacity. Sound waves are applied either during the calcination stage of each CaL cycle or in the carbonation stage. The effect of sound is to intensify the transfer of heat, mass and momentum and is more marked when sound is applied during calcination by promoting CaO regeneration. The application of sound would allow reducing the calcination temperature thereby mitigating the decay of capture capacity with the number of cycles and reducing the energy penalty of the technology.

1 Introduction

The calcium looping (CaL) process is a second generation technology to capture CO_2 by means of cyclic carbonation and calcination of CaO [1–5]. In this process, the gas is passed through a bed of CaO particles at atmospheric pressure in a carbonator reactor operated at around 650 ^{0}C. At this temperature, the kinetics of carbonation is fast enough as required by industrial applications whereas the equilibrium CO_2 concentration is low (around 1% vol.), which allows for a high CO_2 capture efficiency [6]. The carbonated solids are circulated into a second gas-solid reactor (calciner) operated at temperatures above 900 ^{0}C where CaO regeneration takes place. Gas fluidized beds are operated in the fast fluidization regime (gas velocities above m/s) in the case of post-combustion CO_2 capture, which favors the gas-solids contacting efficiency [3]. On the other hand, pre-combustion capture conditions require either fixed or bubbling beds operated at low gas velocities ($\sim$ 1-10 cm/s) [7]. The usually poor thermal conductivity in a fixed bed usually leads to local heating in exothermic reactions (such as carbonation) and local cooling in endothermic reactions (such as calcination), which slow down gas-solid heterogeneous reactions at high temperature. In this work, we investigate the effect of high intensity low frequency sound on the multicycle capture performance of fixed limestone and dolomite beds operated at CaL conditions. If the inertia of a particle in a fluid subjected to a sound wave is large enough to be unmovable by the sound wave, the gas-solid heat/mass transfer can be greatly enhanced because of the development of a convective fluid flow in a boundary layer adjacent to the solid (*acoustic streaming*) [8]. It is therefore envisaged that low frequency sonoprocessing might be a useful technique to promote the gas-solid heat/mass transfer in fixed beds at CaL conditions.

2 Experimental setup and methods

Figure 1 shows the experimental setup used in this work. The reactor consists of a cylindrical quartz vessel (45 mm inner diameter) with a gas distributor made of a quartz plate fitted at its base (2mm thick, 16 to 40 μm pore size). Dry compressed air or a mixture of 15% CO_2 and 85% N_2 is supplied to the inlet port of the reactor by means of two mass flow controllers and a set of valves. For carbonation, a mixture of 15% CO_2+85% N_2 is passed through the reactor while dry compressed air is used for calcination. In either case, a total gas flow of 2000 cm^3/min in standard conditions (25 ^{o}C, 1 atm) is kept fixed by means of the mass flow controllers. The gas exiting the reactor passes through a gas analyzer and a flow meter to monitor its composition. A pressure gauge connected to the inlet port of the reactor is used to measure the total pressure drop across the reactor. An electric signal generator and amplifier are used to excite the loudspeaker to produce the low frequency sound wave that reaches the reactor trough a closed guide. A silicone elastic membrane inside the guide with good sound transmission prevents gas exchange between the reactor and the sound guide. The frequency of the sound was fixed to 130 Hz and the sound level intensity was 157 dB. The temperature is kept at 610 ^{o}C for 45 minutes during the carbonation stage and at 900 ^{o}C for 30 minutes during the calcination stage, with a 15 minutes

⋆e-mail: jmillan@us.es

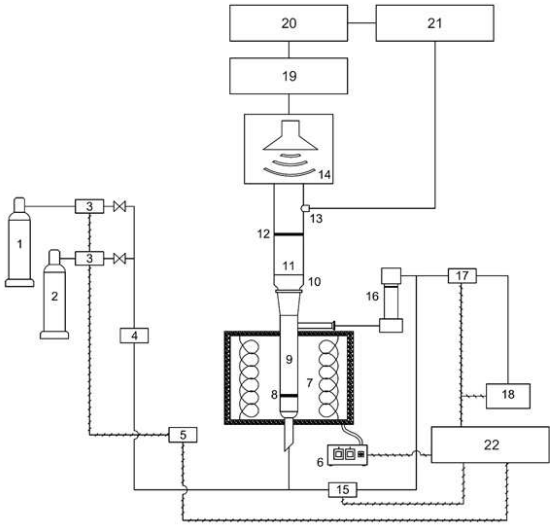

Figure 1. 1: Compressed tank of 15% CO_2 /85 % N_2 vol/vol). 2: Tank of compressed dry air. 3: Mass flow controllers. 4: Safety maximum pressure regulator. 5: Mass flow controller readout. 6: Oven temperature controller. 7: Oven. 8: Quartz fritted filter. 9: Quartz reactor. 10: Teflon adapter. 11: Acoustic waveguide. 12: Silicone elastic membrane. 13: Microphone. 14: Low frequency loudspeaker. 15: Differential pressure transducer. 16: Particle filter. 17: Mass flow meter. 18 CO_2 gas analyzer. 19: Electric amplifier. 20: Electric signal generator. 21: Oscilloscope. 22: Data acquisition and control.

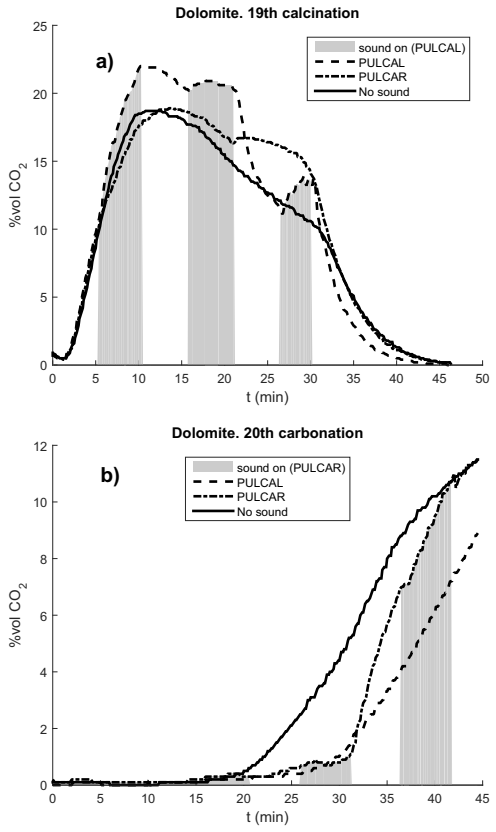

Figure 2. a): CO_2 breakthrough curve during calcination in the 19th cycle. b): CO_2 breakthrough curve during carbonation in the 20th cycle. Both plots are for dolomitic CaO under various operation modes: PULCAR: pulsed sound applied during carbonation; PULCAL pulsed sound applied during calcination.

intermediate period between the calcination and the carbonation stages in which the reactor is vented using dry air while the temperature drops from the calcination to the carbonation temperature. As CaO precursors we have used sieved natural limestone and dolomite particles supplied to us by a local quarry (Taljedi S.L., Gilena, Spain). Only the fraction of particles with mesh sizes d_p in the range 710 μm $\geq d_p \geq$ 425 μm was used. In this range of sizes, the particles have large enough inertia not to be moved by the low frequency sound wave applied. In all the runs, the fresh samples (178 g mass) were initialized by precalcination in-situ at 900 ^{o}C during 30 minutes under dry air.

3 Experimental results and discussion

Figs. 5 and 2 show the time evolution of the CO_2 %vol concentration measured in the effluent gas of the reactor (CO_2 breakthrough curve) during the calcination and the carbonation stages of the 19th and 20th cycles, respectively, for limestone (Fig. 5) and dolomite (Fig. 2). The grey bands in the figures indicate the time span of sound application for the PULCAL data (pulsed sound applied only in calcination stages) and the PULCAR data (pulsed sound applied only in carbonation stages). In the experiments pulsed sound was employed to clearly appreciate the effect of sound application and to allow for refrigeration of the loudspeaker. Thus, the sound generator was turned on for 5 minutes and turned off for another 5 minutes cyclically. As can be seen, the application of high intensity sound waves has a significant effect on enhancing both carbonation and calcination. This effect is more marked for the PULCAL operation mode, in which local maxima of the CO_2 concentration measured in the effluent gas are seen to nearly coincide with the application of sound. Moreover, the effect of sound application is further prolonged to the part of the stage when it is off. As can be seen in Figs. 5 and 2, the CO_2 breakthrough curve obtained for the PULCAL mode remains neatly below the curve obtained for the other two operation modes in the carbonation cycle during the first minutes (although sound is off in PULCAL operation). Likewise the CO_2 breakthrough measured during calcination for the PULCAR mode is well above that measured in the absence of sound (although the sound is off in PULCAR mode). The observation that PULCAL operation causes an increase in the capture rate of CO_2 during the carbonation cycle can be explained by the enhancement of decarbonation in the previous calcination stage, which yields a CaO skeleton with increased porosity and higher available surface area for carbonation. Thus, the PULCAL operation is the mode for which the capture capacity of the sorbent is mostly enhanced.

Fig. 3 and Fig. 4 show the CO_2 breakthrough curves for several carbonation cycles of experimental runs op-

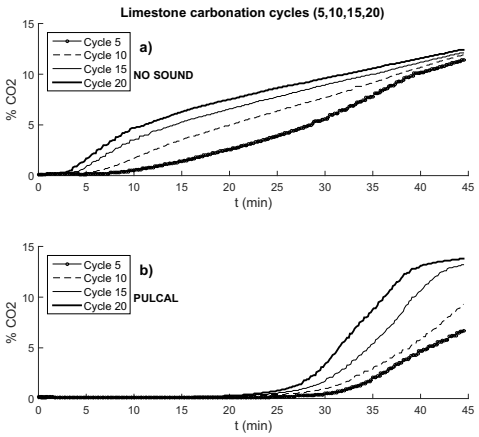

Figure 3. CO_2 breakthrough curves for carbonation cycles under: a) "no sound" and b) PULCAL operation modes for limestone derived CaO.

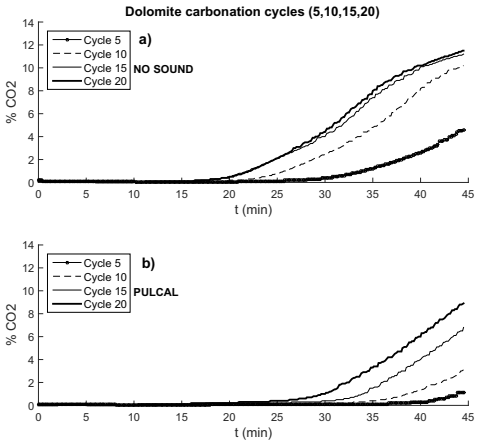

Figure 4. CO_2 breakthrough curves for carbonation cycles under: a) "no sound" and b) PULCAL operation modes for dolomite derived CaO.

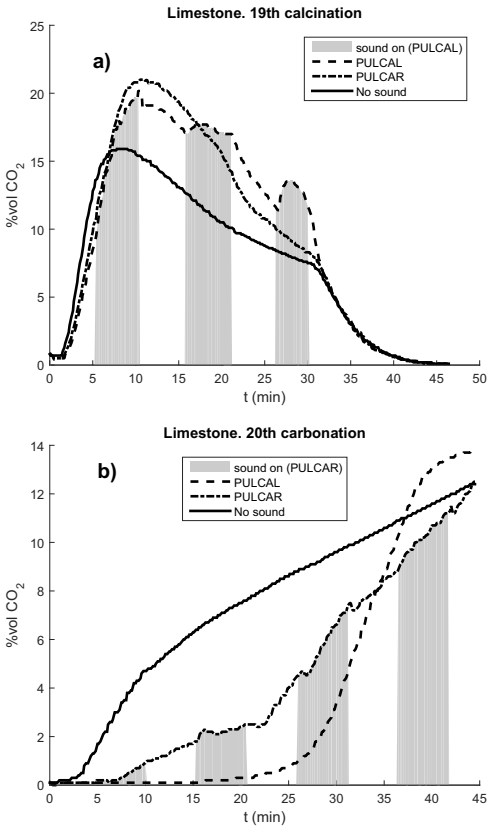

Figure 5. a): CO_2 breakthrough curve during calcination in the 19th cycle. b): CO_2 breakthrough curve during carbonation in the 20th cycle. Both plots are for limestone derived CaO under various operation modes: "No sound": no sound applied; PULCAR: pulsed sound applied during carbonation; PULCAL pulsed sound applied during calcination. Grey bands indicate the time over which high intensity sound is applied.

erated in the PULCAL and "no sound" modes. As may be seen, the effect of PULCAL operation mode on the is much more marked for limestone derived CaO (Fig. 5) than for the dolomitic CaO as might be expected since the MgO inert skeleton would serve already to promote mass/heat transfer in the case of dolomite in the absence of sound as compared to lime.

The total amount of CO_2 captured at each cycle m_{CO_2} has been obtained from the CO_2 breakthrough curves measured in the carbonation stage. It must be taken into account that the MgO, once formed, does not react with CO_2 in the range of temperatures and partial pressures of CO_2 used in our experiments [10] and therefore it remains as inert material. Thus, the maximum theoretical value of the capture capacity for lime is $C_{lim}^{max} = 0.78$ whereas for the dolomitic lime is $C_{dol}^{max} = 0.46$.

Figure 6 shows the capture capacity C as a function of the cycle number measured at the end of the 45 minutes of each carbonation stage. As can be observed, the capture capacity is for both sorbents well below the maximum uptake capacity specially for the first few cycles mainly due to incomplete decarbonation under fixed bed conditions, which severely hinder the transfer of heat and mass. The capture capacity increases in the first cycles as subsequent calcinations allow for a higher degree of decarbonation. After a few cycles, all the available CaO is regenerated during the calcination stage and the capture capacity reaches a maximum, after which it follows a gradual decline with the cycle number arguably caused by a loss of surface area of the sorbent due to sintering in the calcination stages. It is also seen in Fig 6 that the decline of the capture capacity is mitigated for the dolomite derived sorbent as might be expected since the inert MgO present in the dolomite-based sorbent acts as a skeleton that supports the active CaO surface area. Thus, although the dolomite derived sorbent has a smaller percentage of CaO than lime, its capture capacity is larger in accordance with previous results obtained from thermogravimetric tests [11].

The application of high intensity sound would cause an increase in the pressure drop across a particle bed even if the particles are not movable by the sound wave (as is

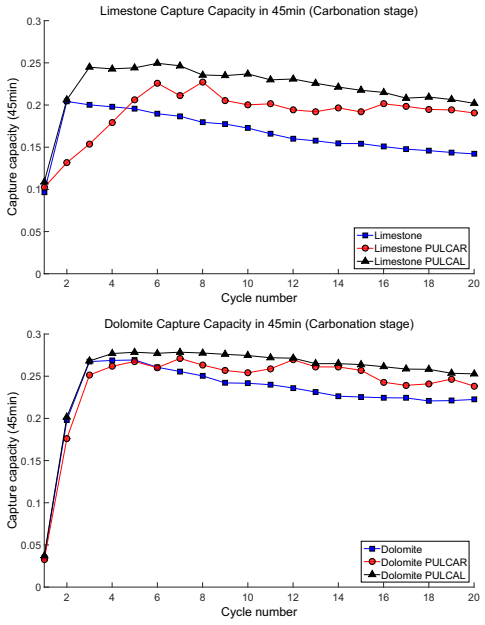

Figure 6. CO_2 capture capacity for limestone and dolomite derived sorbents in the absence of sound and when pulsed sound is applied during the carbonation stage (PULCAR) and in the calcination stage (PULCAL).

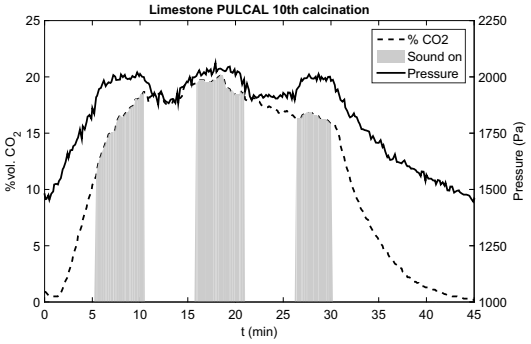

Figure 7. Total pressure drop across the reactor during the 10th calcination cycle of limestone derived CaO in PULCAL operation mode as a function of time together with the %vol CO_2 of the gas leaving the reactor. Grey bands indicate the periods of application of high intensity sound.

the case of our experiments). This increase of pressure drop as due to the relative gas-solid oscillations is caused by the enhancement of viscous dissipation due to acoustic streaming, which consists of the development of a steady rotational gas current in a boundary layer (the so-called Stokes boundary layer) of typical thickness $\delta \sim \sqrt{\nu/\omega}$, where ν is the kinematic gas viscosity and ω is the angular oscillation frequency [8]. Figure 7 shows the time evolution of the pressure drop across the reactor for the 10th calcination stage of limestone derived CaO under PULCAL operation together with the evolution of the % CO_2 in the effluent gas. Remarkably, under PULCAL operation mode, the pressure drop across the reactor follows the same trend than the CO_2 breakthrough curve as the CO_2 released by the sorbent contributes to the net gas flow through the material in the reactor. On top of this general trend, the pressure drop is seen to increase temporarily during the sound pulses.

4 Conclusions

This work sows that application of high-intensity low-frequency sound enhances the capture capacity of natural limestone and dolomite fixed beds along carbonation/calcination cycles due to acoustic streaming resulting from the frictional dissipation of energy in a boundary layer nearby the solids. Acoustic streaming promotes heat and mass transfer thus accelerating both carbonation and calcination. This effect is more marked when the pulsed sound is applied during the calcination stage arguably due to the relatively higher temperature, which promotes further the gas viscosity and therefore acoustic streaming.

Acknowledgements

This work was supported by the Spanish Government Agency Ministerio de Economia y Competitividad and FEDER Funds (Contract CTQ2014-52763-C2-2-R).

References

[1] V. Manovic, E.J. Anthony, J. Phys. Chem. A **114**, 3997 (2010)
[2] W. Wang, S. Ramkumar, D. Wong, L.S. Fan, Fuel **92**, 94 (2012)
[3] B. Arias, M.E. Diego, J.C. Abanades, M. Lorenzo, L. Diaz, D. Martínez, J. Alvarez, A. Sanchez-Biezma, Int. J. Greenh. Gas Control **18**, 237 (2013)
[4] I. Martínez, G. Grasa, R. Murillo, B. Arias, J.C. Abanades, Energy Fuels **26**, 1432 (2012)
[5] A. Perejón, L.M. Romeo, Y. Lara, P. Lisbona, A. Martínez, J.M. Valverde, Appl. Energy **162**, 787 (2016)
[6] C. Ortiz, R. Chacartegui, J. Valverde, J. Becerra, Appl. Energy **169**, 408 (2016)
[7] K. K. Johnsen, H. Ryu, J. Grace, C. Lim, Chem. Eng. Sci. **61**, 1195 (2006)
[8] J. Valverde, Eur. Phys. J. E **38**, 38 (2015)
[9] J. Readman, B. Richard, Phys. Chem. Chem. Phys. **7**, 1214 (2005)
[10] J. Valverde, P. Sanchez-Jimenez, L. Perez-Maqueda, Appl. Energy **138**, 202 (2015)